Optimization of Reactive Power Distribution in Series PV-Battery-Hybrid Systems

Pan, Yiwei; Sangwongwanich, Ariya; Yang, Yongheng; Blaabjerg, Frede

Published in:
Proceeding of 2020 IEEE Energy Conversion Congress and Exposition (ECCE)

DOI (link to publication from Publisher):
10.1109/ECCE47101.2021.9595659

Publication date:
2021

Document Version
Accepted author manuscript, peer reviewed version

Optimization of Reactive Power Distribution in Series PV-Battery-Hybrid Systems

Yiwei Pan*, Ariya Sangwongwanich*, Yongheng Yang+, and Frede Blaabjerg*
*Department of Energy Technology, Aalborg University, Aalborg 9220, Denmark
+College of Electrical Engineering, Zhejiang University, Hangzhou 310027, China
E-mails: ypa@et.aau.dk, ars@et.aau.dk, yang_yh@zju.edu.cn, fbl@et.aau.dk

***Abstract*— Series topologies have been gaining interest in photovoltaic-battery-hybrid (PVBH) applications. In previous research, the reactive power contribution from PVBH systems is distributed in a way to maintain the apparent power of all converters at the same level. However, the prior-art strategies cannot ensure optimal reactive power distribution, as the calculated reactive power references are not the analytical optimal solutions. In most cases, the apparent power of certain converters can be higher than others. This will lead to the overloading of certain converters and even the power curtailment of PV converters in extreme cases. To improve the performance of the reactive power distribution, an optimized reactive power distribution method based on the particle swarm optimization (PSO) algorithm is proposed in this paper. By doing so, the optimal reactive power reference for each converter can be obtained, and thus, preventing the potential overloading of certain converters. Experimental results have validated the effectiveness of the proposed solution.**

***Keywords*—power control, power distribution, power optimization, PV-battery systems, series-connected converters.**

I. Introduction

With the development of distributed generation (DG), series topologies such as cascaded H-bridge (CHB) converters have become an attractive solution for DG applications [1]-[5]. With the series structures, low-voltage DG units can be directly interfaced to separate DC rails of series converters, thus avoiding the use of additional DC/DC stages [1]-[4]. This will bring several benefits like reduced cost and improved efficiency. On the other hand, the energy storage elements such as batteries can also be equipped to compensate for the power variations of DG systems and enhance the power quality [5]-[11]. Accordingly, the coordinated operation of PV panels and batteries using series topologies has been studied recently [6]-[11].

The configuration of a typical series PVBH system is shown in Fig. 1, where a 3-cell series PVBH system is realized by two PV converters and one battery converter. For series PVBH systems, the active power of each PV converter is mainly determined by the maximum power point tracking (MPPT) control, while the battery converters provide/absorb surplus power according to the load demand. This means that the loading of individual converters can be unequal in most cases depending on the power production of the PV panels [6]-[11]. When there is reactive power demand for the series system, one solution is to employ one converter to provide all required reactive power, as introduced in [12]. However, this approach

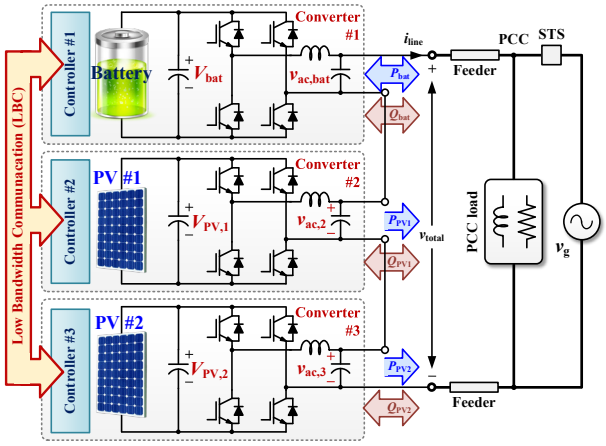

Fig. 1. System schematic of a 3-cell series PVBH system, where $v_{ac,k}$ and $v_{ac,bat}$ are the AC voltages of the k^{th} converter cell and the battery cell, P_{PVk} and Q_{PVk} refer to the active and reactive power of the k^{th} PV converter, P_{bat} and Q_{bat} are the active and reactive power of the battery converter, $V_{PV,m}$ and V_{bat} are the DC voltages of PV #*m* and the battery, respectively, v_{total} is the output voltage of the system, PCC represents the point of common coupling, and STS stands for static transfer switch.

is not feasible, as the selected converter will easily suffer from overloading when a large amount of reactive power is required. To improve the utilization of the power capacity of all converters, a distributed power management approach was proposed in [8], where the reactive power is distributed among all converters. Nevertheless, the power factors (PFs) of individual converters in [8] are always kept consistent with the PF of the entire system, which means that the reactive power is distributed in proportion to the active power of each PV converter. In other words, the PV converter with more active power will also have to provide more reactive power, which will increase the uneven loading among all converters. Therefore, the approach in [8] may not ensure optimal reactive power distribution in series PVBH systems.

A more suitable reactive power distribution approach is to distribute the reactive power in a way to balance the apparent power and thereby the loading of all converters. More specifically, the converter with more active power should provide less reactive power in order to balance the loading among different cells. To achieve this goal, several reactive power distribution strategies have been developed for series PVBH systems [9]-[11]. In [9] and [10], the reactive power was distributed proportionally with respect to the surplus power

capacity of each PV converter. However, the strategies in [9] and [10] cannot ensure optimal load balancing among all converters, as the converter with the largest active power may still be required to provide a large amount of reactive power, especially when the total active power for the entire system is small. In [11], a distributed reactive power sharing approach was developed, where the reactive power reference is calculated based on the local active power and the total power information. Due to the limited power information obtained by each converter, it is assumed that other converters are synthesizing the total ac voltage with the minimum ac voltage amplitudes [11]. Nevertheless, this assumption is not accurate in practice, as the voltages of other converters cannot exactly be the assumed voltages with minimum amplitudes. Therefore, the approach in [11] cannot achieve the optimal reactive power distribution as well. In fact, according to the experimental results in [9]-[11], the total apparent power is only approximately balanced among all converters, and the total loading of certain converters (e.g., apparent power) can be higher than others. This means that certain converters are still under the risk of overloading or over-modulation, which may adversely affect the system performance, e.g., accelerated aging of certain converters [13] and active power curtailment of PV converters [8].

To improve the reactive power distribution performance of series PVBH systems, a reactive power distribution optimization method is thus proposed in this paper. Firstly, the cost function is developed to obtain the optimum reactive power reference for each converter. Then, a particle swarm optimization (PSO) method is employed to find the optimal solution for the reactive power distribution. Experimental results are provided to verify the effectiveness of the proposed method, and evaluate its dynamic performance. Despite a large amount of calculations, each optimization iteration can be finished in several milliseconds with an ordinary digital signal processor (DSP), which indicates that the proposed PSO-based algorithm can be continuously executed online.

II. Proposed Optimal Reactive Power Distribution

For simplicity, only one battery converter is considered for an n-cell series PVBH system as an example. As discussed previously, the active power of (n−1) PV converters (denoted as P_1, … P_{n-1}, respectively) are determined by the MPPT control, while the total active and reactive power of the system are determined by the load/grid demand. Then, the objective of the reactive power distribution is to find a set of reactive power $\{Q_1, \dots Q_{n-1}\}$ with the given power information $\{P_1, \dots P_{n-1}, P_{total}, Q_{total}\}$, to minimize: 1) the differences between the apparent power of individual converters, and 2) the sum of the apparent power for all converters. The reactive power should subject to $0 \le Q_k \le Q_{total}$, where $k = 1, \dots n$, being the converter index number. However, it is challenging to analytically calculate the optimal set of reactive power references through traditional analytical methods, especially when the number of series converters is high. Therefore, the PSO method is employed in this paper to solve the optimization problem, which is suitable to obtain the numerical solutions for continuous nonlinear functions [14], [15]. Accordingly, the cost function of the optimization problem can be designed as

$$g = p_1\sqrt{\frac{1}{n}\sum_{k=1}^{n}\left(S_k - \overline{S}\right)^2} + p_2\sum_{k=1}^{n}S_k \tag{1}$$

where S_k refers to the apparent power of the k^{th} converter, $\overline{S}$ is the average apparent power for all converters ($\overline{S} = (1/n)\sum_{k=1}^{n} S_k$), and p_1 and p_2 are two weighting factors. If a set of $\{Q_1, \dots Q_{n-1}\}$ is found to minimize the function g, it can be regarded as the best reactive power distribution command. The PSO-based algorithm is detailed as follows:

1) Initialize the positions and velocities for a total number of M particles. The positions and velocities should within the feasible region. For instance, for the m^{th} particle, its initial position $\vec{Q}_m^0$ and velocity $\vec{v}_m^0$ are defined as

$$\vec{Q}_m^0 = \begin{bmatrix} Q_{m,1}^0 \\ Q_{m,2}^0 \\ \dots \\ Q_{m,n-1}^0 \end{bmatrix} = \begin{bmatrix} rand\left([0, Q_{total}]\right) \\ rand\left([0, Q_{total}]\right) \\ \dots \\ rand\left([0, Q_{total}]\right) \end{bmatrix} \tag{2}$$

and

$$\vec{v}_m^0 = \begin{bmatrix} v_{m,1}^0 \\ v_{m,2}^0 \\ \dots \\ v_{m,n-1}^0 \end{bmatrix} = \begin{bmatrix} rand\left([-v_{max}, v_{max}]\right) \\ rand\left([-v_{max}, v_{max}]\right) \\ \dots \\ rand\left([-v_{max}, v_{max}]\right) \end{bmatrix} \tag{3}$$

where $rand([a,b])$ refers to a random number within the range of $[a,b]$, and v_{max} is the pre-defined maximum velocity.

2) Calculate the g-values for all particles using (1). Then, store the historical optimal position (with minimum g) for each particle, as well as the historical optimal position among all particles. The two positions are denoted as $\vec{Q}_{m,best}^{\alpha}$ and $\vec{Q}_{g,best}^{\alpha}$, where the superscript "α" indicates that the value is calculated in the α^{th} cycle of the optimization iteration.

3) Update the positions and velocities of all particles using

$$\begin{aligned} \vec{v}_m^{\alpha+1} = {} & \omega \cdot \vec{v}_m^{\alpha} + \phi_p \cdot rand\left([0,1]\right) \cdot \left(\vec{Q}_{m,best}^{\alpha} - \vec{Q}_m^{\alpha}\right) \\ & + \phi_g \cdot rand\left([0,1]\right) \cdot \left(\vec{Q}_{g,best}^{\alpha} - \vec{Q}_m^{\alpha}\right) \end{aligned} \tag{4}$$

and

$$\vec{Q}_m^{\alpha+1} = \vec{Q}_m^{\alpha} + \vec{v}_m^{\alpha+1} \tag{5}$$

where ω, ϕ_p and ϕ_g are three predefined constant values. Then, repeat the procedure 2) and 3) until the iteration reaches the maximum cycle index α_{max}.

4) After the final cycle of iteration, $\vec{Q}_{g,best}^{\alpha}$ is obtained as the reactive power references for individual converters.

To obtain the optimal set of reactive power references, the number of particles and the total rounds of iterations should be

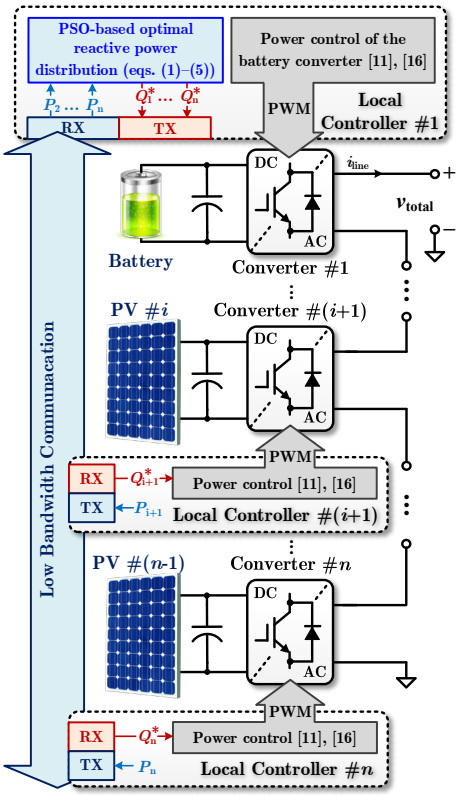

Fig. 2. Overall control diagram of an n-cell series PVBH system with the proposed reactive power optimization, where Q_k^* is the reactive power reference for the k^{th} converter, and TX and RX represent transport and receive, respectively.

high, which means that the calculation can be time-consuming due to heavy computation. However, the dynamics of the power distribution among the series converters are relatively slow in practice, i.e., limited by the MPPT control, which is usually in the range of 50 to 200 milliseconds according to the results in [11] and [16]. This indicates that a fast optimization is not necessarily required. In other words, if the optimization can be accomplished within every 50 milliseconds, the proposed methods will be sufficient to meet the dynamic requirement of the reactive power distribution in series PVBH systems. The dynamic performance of the proposed method will be detailed in the next section.

The PSO-based optimization algorithm can be implemented in any one of the local controllers. Fig. 2 demonstrates the control diagram of the system with the proposed reactive power optimization, where it is implemented in the controller of the battery converter. As it can be observed form Fig. 2, the proposed algorithm relies on the low-bandwidth communication (LBC) to collect active power information and distribute reactive power reference of each converter. Compared with the reactive power distribution strategy in [11], the only added data for communication are the active power information of individual converters, which have very slow dynamics, as mentioned previously. Thus, the LBC can still be sufficient to achieve the proposed reactive power optimization.

As the PSO algorithm may fall into local optimum within limited rounds of iterations, the obtained reactive power

TABLE I
PARAMETERS OF THE 3-CELL PVBH CONVERTER WITH THE PROPOSED CONTROL METHOD.

Circuit parameter	Value
PV rated power	800 W
PV maximum power point voltage	260 V
Nominal grid frequency ω_{nom}	$2\pi \cdot 50$ rad/s
Nominal grid voltage $V_{g,nom}$ (RMS)	230 V
Output LC filter of one cell	1.8 mH / 30 μF
Nominal voltage of the battery	192 V
DC link capacitor for PV converters	1360 μF
Basic control parameters	**Value**
MPPT sampling ferquency	5 Hz
MPPT step-size	6 V
Controller sampling frequency	10 kHz
Communication baud rate	9600 b/s
Control parameters for the power distribution	**Value**
Weighting factors for optimization	$p_1 = 0.3$, $p_2 = 0.7$
Constants for the PSO algorithm	$\omega = 0.5$, $\phi_p = \phi_g = 0.2$
Total number of particles M	100
Maximum cycle of iteration α_{max}	200
Reactive power distribution coefficient h [11]	2.8

references may not be the best solutions [14]. Even if the given $\{P_1, \ldots P_{n-1}, P_{total}, Q_{total}\}$ remain consistent, the obtained reactive power distribution $\{Q_1, \ldots Q_{n-1}\}$ may be different in every optimization round, which will lead to unwanted oscillations on the reactive power of each converter. To solve this issue, one solution is to increase the total number of either particles or iterations. However, this will significantly increase the computation burdens. A cost-effective way is to initialize the position of any one particle as $\{Q_1, \ldots Q_{n-1}\}$ in the last optimization round. By doing so, the optimal or suboptimal solution calculated in the last optimization round will be involved in the next round of optimization. Therefore, even if the optimal reactive power command is not obtained after one round of optimization, it will be acquired in the future rounds. Once the optimal solution is obtained, it will not be changed as long as $\{P_1, \ldots P_{n-1}, P_{total}, Q_{total}\}$ remain consistent. In addition, even $\{P_1, \ldots P_{n-1}, P_{total}, Q_{total}\}$ vary, this modified initialization will not affect the dynamic performance of the proposed method.

III. EXPERIMENTAL RESULTS

To validate the effectiveness of the proposed optimization method, experiments were performed on a grid-connected 3-cell PVBH system, with its configuration shown in Fig. 1. The photo of the experimental prototype is shown in Fig. 3. Three Infineon FS50R12KT4_B15 IGBT modules were employed to assemble the experimental prototype. Two programmable DC power supplies were used to emulate the two PV modules, and one Delta Elektronika SM330 DC power supply in parallel with a resistor bank was adopted to mimic the battery. Three TMS320F28335 DSPs were employed as local controllers for individual converters, which were interlinked with RS-485 serial communication. The parameters of the experiments are shown in Table I, and the results are provided in Figs. 4-9. The reactive power distribution method in [11] was implemented in the experiment for comparison.

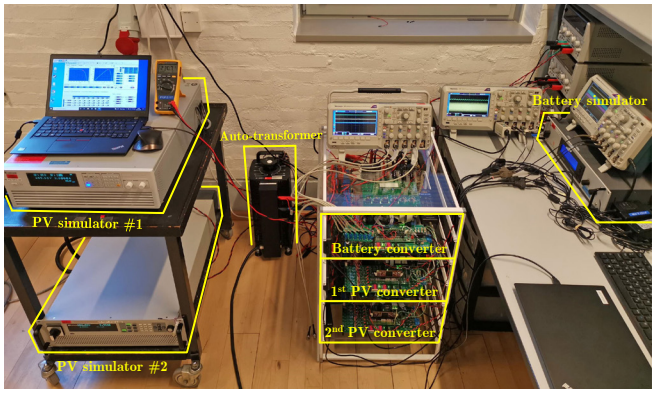

Fig. 3. Experimental prototype of the 3-cell series PVBH systems.

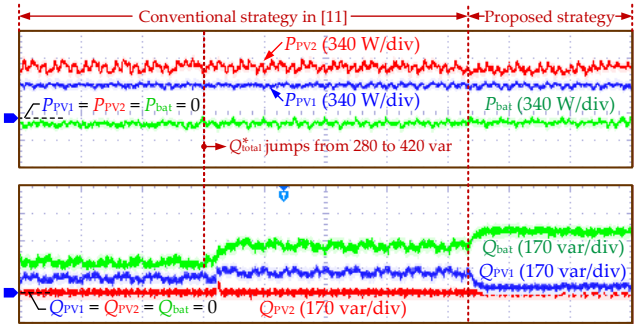

Fig. 4. Power control performance of the reactive power distribution strategy in [11] and the proposed optimization method (time [2 s/div]).

Test 1: First, the reactive power distribution performance of the proposed method is compared with the strategy in [11], and the results are shown in Figs. 4-6. As shown in Fig. 4, in the initial stage, a total power being 950 W and 280 var is required for the series system. The two PV converters are operating at their maximum power points (MPPs), with their DC voltages being oscillating around 260 V as shown in Fig. 5, and active power being 610-W and 410-W for the 1st and 2nd PV converter, respectively. The surplus 70-W power is absorbed by the battery converter. Due to the reactive power distribution strategy in [11], the reactive power is distributed according to the active power of each converter, with approximately 85 var and 0 var from the 1st and 2nd PV converter, respectively, while the remaining 195-var power is provided by the battery converter. The apparent power for each converter can thus be calculated, being 419 VA, 610 VA and 207 VA for the 1st, 2nd PV converter and the battery converter. This result can be confirmed by Fig. 6, where the amplitude of the output ac voltage for each converter is proportional to its apparent power, and the amplitude of $v_{ac,PV1}$ is almost twice than that of $v_{ac,bat}$. Clearly, although the reactive power is distributed among all converters depending on their active power loading according to the strategy in [11], the distribution is not optimized as the battery converter is less loaded.

Then, the required total reactive power is increased to 420 var. Consequently, the reactive power of the 1st PV converter increases to be around 130 var, while it remains zero for the 2nd PV converter, and the remaining 290-var reactive power is provided by the battery converter. The MPPT operation of the two PV converters is not affected, with their

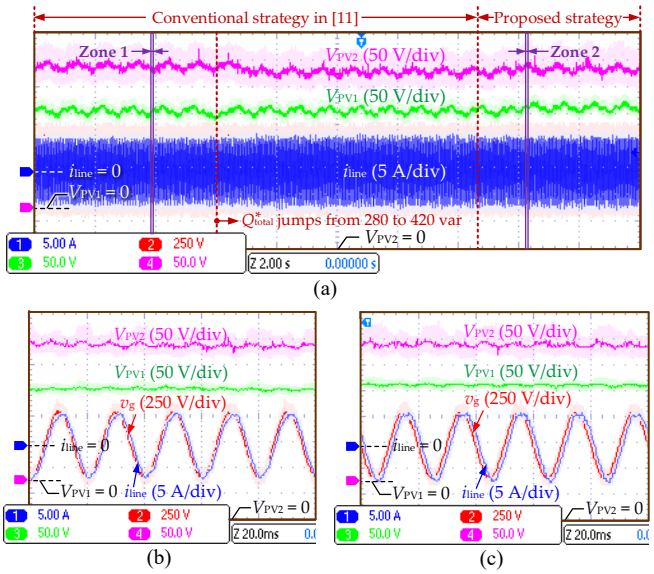

Fig. 5. Current and voltage responses of the system in Test 1 (the time scale is 2 s/div for Fig. 5(a), and 20 ms/div for Figs. 5(b) and (c)): (a) PV voltages and grid current, (b) zoomed-in plot of Zone 1 in Fig. 5(a), and (c) zoomed-in plot of Zone 2 in Fig. 5(a), where v_g is the grid voltage.

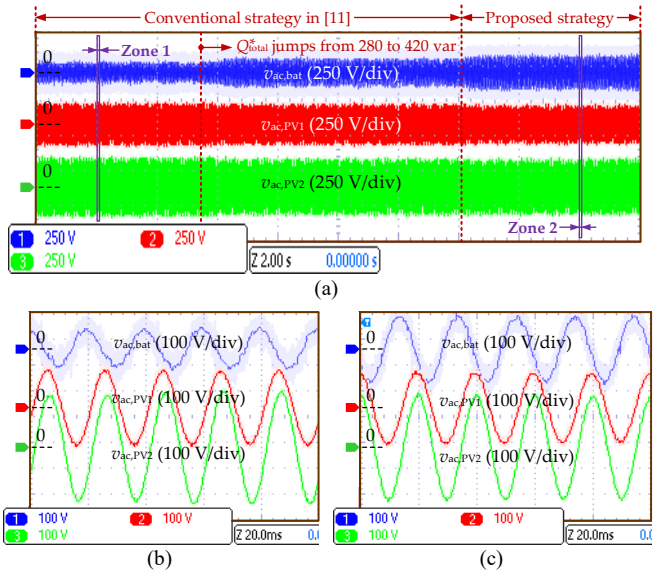

Fig. 6. Voltage responses of individual converters in Test 1 (the time scale is 2 s/div for Fig. 6(a), and 20 ms/div for Figs. 6(b) and (c)): (a) PV voltages and grid current, (b) zoomed-in plot of Zone 1 in Fig. 6(a), and (c) zoomed-in plot of Zone 2 in Fig. 6(a), where $v_{ac,PV1}$ and $v_{ac,PV2}$ are the output ac voltage of the 1st and 2nd PV converters, respectively.

DC voltages being around 260 V, as shown in Fig. 4, and their power unchanged. The apparent power can be calculated as 430 VA, 610 VA, and 298 VA for the 1st, 2nd PV converter and the battery converter. It can be noticed that although the battery converter provides most reactive power, it is still less loaded compared with the PV converters.

The proposed reactive power optimization strategy is enabled afterwards. As it can be observed from Fig. 4, the active power of all converters remains unchanged, while the reactive power becomes 30 var, 0 var and 390 var for the 1st, 2nd PV converter and the battery converter, and the corresponding

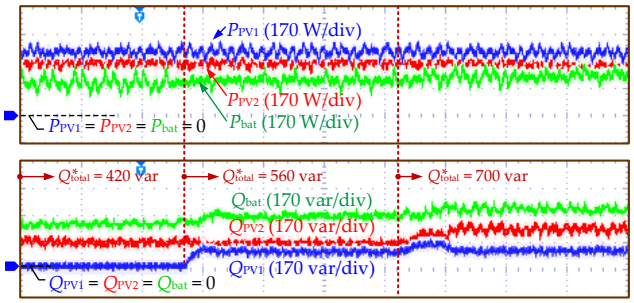

Fig. 7. Reactive power step response of the proposed optimization method (time [2 s/div]).

apparent power can be calculated as 411 VA, 610 VA and 396 VA, respectively. Compared with the former reactive power distribution performance using the strategy in [11], the loading of all converters are more balanced with the proposed strategy.

Test 2: The dynamic performance of the proposed reactive power optimization strategy is demonstrated in Figs. 7-9. Initially, approximately 410-W, 330-W and 210-W active power is provided by the 1st, 2nd PV converter and the battery converter, respectively. The two PV converters are operating around their MPPs, with their DC voltages being around 260 V, as shown in Fig. 8. Since the battery converter has the smallest active power loading among all converters, it provides most of the total reactive power, being 270 var, while the remaining 150-var reactive power is provided by the 2nd PV converter. The apparent power can be obtained as 410 VA, 362 VA, and 342 VA for the two PV converters and the battery converter, where it can be noticed that the 2nd PV converter and the battery converter have similar loading. Then, the required total reactive power is increased to 560 var. As a result, the reactive power of the two PV converters and the battery converter is around 90 var, 150 var, and 320 var, respectively, with their apparent power being 420 VA, 362 VA and 383 VA, respectively. It can be noticed that the power loading for all the three converters are approximately balanced. Finally, the required total reactive power is increased to 700 var. After the reactive power step change, it takes about 1.6 s for the reactive power distribution to reach the new steady state, where the reactive power is around 95 var, 240 var, and 365 var for the 1st, 2nd PV converters and the battery converter, respectively. Due to higher conduction losses caused by the increase on the amplitude of the line current, the active power of the 1st and 2nd PV converter is slightly decreased to 395 W and 315 W, respectively, while the active power from the battery converter is increased to 240 W to provide the total required 950-W power. With the above, the apparent power can be obtained as 406 VA, 396 VA and 437 VA. Thus, it can be observed that the reactive power is distributed among all converters to equalize their loading. This result can also be confirmed by Fig. 9, where the ac voltage amplitudes of all converters are almost equal.

In Test 2, the proposed reactive power optimization is continuously executed online. According to the tests, it takes about 12 milliseconds for the DSP to accomplish one round of optimization for a 3-cell series PVBH system. The bandwidth for the reactive power optimization is similar with that of the LBC (9600 b/s according to Table I), and is much faster than the MPPT operation. This indicates that the proposed PSO-based optimization method will not limit the control bandwidth of the power distribution control, which is sufficient to meet the requirements of fast power control, even for systems with more cascaded converters.

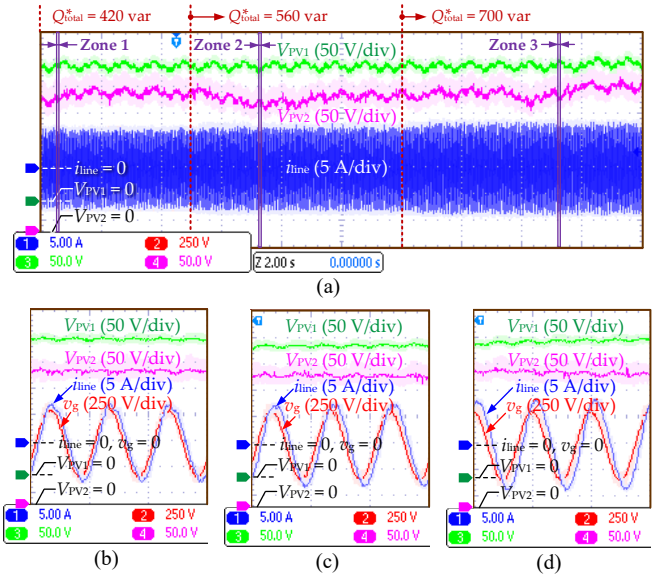

Fig. 8. Current and voltage responses of the system in Test 2 (the time scale is 2 s/div for Fig. 8(a), and 20 ms/div for Figs. 8(b) and (c)): (a) PV voltages and grid current, (b) zoomed-in plot of Zone 1 in Fig. 8(a), and (c) zoomed-in plot of Zone 2 in Fig. 8(a).

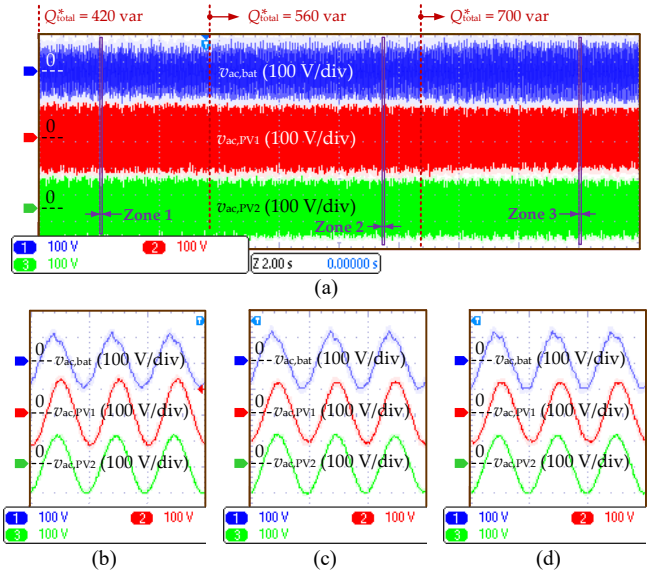

Fig. 9. Voltage responses of individual converters in Test 2 (the time scale is 2 s/div for Fig. 9(a), and 20 ms/div for Figs. 9(b) and (c)): (a) PV voltages and grid current, (b) zoomed-in plot of Zone 1 in Fig. 9(a), (c) zoomed-in plot of Zone 2 in Fig. 9(a), and (d) zoomed-in plot of Zone 3 in Fig. 9(a).

IV. Conclusions

To improve the power balancing performance of series PVBH systems, an optimization method in terms of reactive power distribution was proposed in this paper. Based on the PSO algorithm, the optimal reactive power references for individual converters can be obtained, with which the apparent

power can be balanced to the largest extent. Owing to this, the unbalanced loading among converters, as well as the overloading risk for certain converters induced by the non-optimal reactive power distribution in prior-art methods can be alleviated. Experimental results have demonstrated the effectiveness of the proposed method in terms of improving the load balancing of PV and battery converters, and verified the feasibility of the proposed method in terms of online execution.

REFERENCES

[1] Y. Yang, K. A. Kim, F. Blaabjerg, and A. Sangwongwanich, *Advances in Grid-Connected Photovoltaic Power Conversion Systems*, Publisher: Woodhead Publishing, 2018.

[2] B. Xiao, L. Hang, J. Mei, C. Riley, L. M. Tolbert, and B. Ozpineci, "Modular cascaded H-bridge multilevel PV inverter with distributed MPPT for grid-connected applications," *IEEE Trans. Ind. Appl*., vol. 51, no. 2, pp. 1722-1731, Mar./Apr. 2015.

[3] J. He, Y. Li, C. Wang, Y. Pan, C. Zhang, and X. Xing, "Hybrid microgrid with parallel- and series-connected microconverters," *IEEE Trans. Power Electron*., vol. 33, no. 6, pp. 4817-4831, June 2018.

[4] L. Zhang, K. Sun, Y. W. Li, X. Lu, and J. Zhao, "A distributed power control of series-connected module-integrated inverters for PV grid-tied applications," *IEEE Trans. Power Electron*., vol. 33, no. 9, pp. 7698-7707, Sept. 2018.

[5] B. Xu, H. Tu, Y. Du, H. Yu, H. Liang, and S. Lukic, "A distributed control architecture for cascaded H-bridge converter with integrated battery energy storage," *IEEE Trans. Ind. Appl*., vol. 57, no. 1, pp. 845-856, Jan.-Feb. 2021.

[6] H. Liao, X. Zhang, and X. Hou, "A decentralized control of series-connected PV-ES inverters with MPPT and virtual inertia functionality," in *Proc. IEEE APEC*, Mar. 2020, pp. 3221-3224.

[7] N. Kim and B. Parkhideh, "Control and operating range analysis of an AC-stacked PV inverter architecture integrated with a battery," *IEEE Trans. Power Electron*., vol. 33, no. 12, pp. 10032-10037, Dec. 2018.

[8] S. Das, I. U. Nutkani, and C. Teixeira, "Autonomous power management of series-parallel hybrid microgrid," in *Proc. IEEE ICPES*, 2019, pp. 1-6.

[9] Y. Pan, C. Zhang, S. Yuan, A. Chen, and J. He, "A decentralized control method for series connected PV battery hybrid microgrid," in *Proc. ITEC Asia-Pacific*, Aug. 2017, pp. 1–6.

[10] Q. Zhang and K. Sun, "A flexible power control for PV-battery hybrid system using cascaded H-bridge converters," *IEEE J. Emerg. Sel. Topics Power Electron*., vol. 7, no. 4, pp. 2184-2195, Dec. 2019.

[11] Y. Pan, A. Sangwongwanich, Y. Yang, and F. Blaabjerg, "Distributed control of islanded series PV-battery-hybrid systems with low communication burden," *IEEE Trans. Power Electron.*, vol. 36, no. 9, pp. 10199-10213, Sept. 2021.

[12] H. Jafarian, R. Cox, J. H. Enslin, S. Bhowmik, and B. Parkhideh, "Decentralized active and reactive power control for an AC-stacked PV inverter with single member phase compensation," *IEEE Trans. Ind. Appl*., vol. 54, no. 1, pp. 345-355, Jan.-Feb. 2018.

[13] Y. Ko, M. Andresen, G. Buticchi, and M. Liserre, "Power routing for cascaded H-bridge converters," *IEEE Trans. Power Electron*., vol. 32, no. 12, pp. 9435-9446, Dec. 2017.

[14] Y. Del Valley, G. K. Venayagamoorthy, S. Mohagheghi, J.-C. Hernandez, and R. G. Harley, "Particle swarm optimization: Basic concepts, variants and applications in power systems," *IEEE Trans. Power Del*., vol. 12, no. 2, pp. 171–195, Apr. 2008.

[15] T. Xu and F. Gao, "Global synchronous pulse width modulation of distributed inverters," *IEEE Trans. Power Electron*. Vol. 31, no. 9, pp. 6237-6253, Sept. 2016.

[16] Y. Pan, A. Sangwongwanich, Y. Yang, and F. Blaabjerg, "Flexible power control of distributed grid-connected series-photovoltaic-battery systems," in *Proc. IEEE APEC*, Jun. 2021, pp. 1-8.